Kaon and Pion Production in Central Au+Au Collisions at $\sqrt{s_{NN}} = 62.4$ GeV[☆]

I.C.Arsene[*,k], I.G.Bearden[f], D.Beavis[a], S.Bekele[j,1], C.Besliu[i], B.Budick[e], H.Bøggild[f], C.Chasman[a], C.H.Christensen[f], P.Christiansen[f,4], H.H.Dalsgaard[f], R.Debbe[a], J.J.Gaardhøje[f], K.Hagel[g], H.Ito[a], A.Jipa[i], E.B.Johnson[j,2], C.E.Jørgensen[f,6], R.Karabowicz[d], N.Katrynska[d], E.J.Kim[j,3], T.M.Larsen[f], J.H.Lee[a], G.Løvhøiden[k], Z.Majka[d], M.J.Murray[j], J.Natowitz[g], B.S.Nielsen[f], C.Nygaard[f], D.Pal[j], A.Qviller[k], F.Rami[b], C.Ristea[f], O.Ristea[i], D.Röhrich[h], S.J.Sanders[j], P.Staszel[d], T.S.Tveter[k], F.Videbæk[a,8], R.Wada[g], H.Yang[h,7], Z.Yin[h,5], and I.S.Zgura[c]

[a]*Brookhaven National Laboratory, Upton, New York, USA*
[b]*Institut Pluridisciplinaire Hubert Curien et Université de Strasbourg, Strasbourg, France*
[c]*Institute of Space Science,Bucharest-Magurele, Romania*
[d]*M. Smoluchowski Inst. of Physics, Jagiellonian University, Krakow, Poland*
[e]*New York University, New York, USA,*
[f]*Niels Bohr Institute, University of Copenhagen, Copenhagen, Denmark*
[g]*Texas A&M University, College Station, Texas, USA*
[h]*University of Bergen, Department of Physics and Technology, Bergen, Norway*
[i]*University of Bucharest, Romania*
[j]*University of Kansas, Lawrence, Kansas, USA*
[k]*University of Oslo, Department of Physics, Oslo, Norway*

Abstract

Invariant p_T spectra and rapidity densities covering a large rapidity range ($-0.1 < y < 3.5$) are presented for $\pi^\pm$ and $K^\pm$ mesons from central Au+Au collisions at $\sqrt{s_{NN}} = 62.4$ GeV. The mid-rapidity yields of meson particles relative to their anti-particles are found to be close to unity ($\pi^-/\pi^+ \sim 1$, $K^-/K^+ \sim 0.85$) while the anti-proton to proton ratio is $\bar{p}/p \sim 0.49$. The rapidity dependence of the π^-/π^+ ratio is consistent with a small increase towards forward rapidities while the K^-/K^+ and $\bar{p}/p$ ratios show a steep decrease to ~ 0.3 for kaons and 0.022 for protons at $y \sim 3$. It is observed that the kaon production relative to its own anti-particle as well as to pion production in wide rapidity and energy ranges shows an apparent universal behavior consistent with the baryo-chemical potential, as deduced from the $\bar{p}/p$ ratio, being the driving parameter.

Key words: heavy ion collisions, strangeness enhancement, baryon chemical potential
PACS: 25.75q

Introduction

As the collision energy has increased with the advent of new relativistic heavy-ion accelerators, from AGS energies ($\sqrt{s_{NN}} \leq 4.9$ GeV) to those achieved with the SPS ($\sqrt{s_{NN}} \leq 17.3$ GeV) and recently with RHIC ($\sqrt{s_{NN}} \leq 200$ GeV), the system created in heavy-ion collisions has been found to evolve from one that is baryon rich to one dominated by mesons [1, 2, 3, 4]. This change is evident in the increase of central rapidity densities of emitted pions and kaons accompanied by the simultaneous shift of the net-baryon peak one or two units of rapidity down from beam rapidity. Due to this shift, the net-baryon peak gradually moves from mid-rapidity (AGS and SPS) [5, 6] towards high rapidity (RHIC) [7], leaving a relatively net-baryon poor region at mid-rapidity at the highest RHIC energy.

At AGS energies, the observed ratio of strange particles to pions in A+A collisions is larger than that measured in either p+p or p+A collisions and this ratio increases significantly with beam energy [2, 8, 9]. This behavior is understood within cascade models as arising from hadronic rescatterings involving heavy baryon resonances [10, 11]. In the SPS energy range it is conjectured [12] that the nuclear fireball undergoes a phase transition from bound hadronic matter to a deconfined quark-gluon plasma state (QGP). This conjecture is supported by the observation that excitation functions of the K^+/π^+, Λ/π, and Ξ^-/π ratios at mid-rapidity are found to peak

[☆]The BRAHMS Collaboration
[*]Corresponding Author. *e-mail: i.c.arsene@fys.uio.no*(I.C.Arsene)
Present Address: ExtreMe Matter Institute EMMI, GSI Helmholtzzentrum für Schwerionenforschung GmbH, Darmstadt, Germany
[1]Present Address: Dept of Physics, Tennessee Tech University,Cookeville, Tennessee
[2]Present address: Radiation Monitoring Devices, Cambridge, MA, USA
[3]Present address: Division of Science Education, Chonbuk National University, Jeonju, Korea
[4]Present Address: Div. of Experimental High-Energy Physics, Lund University, Lund, Sweden
[5]Present Address: Institute of Particle Physics, Huazhong Normal University,Wuhan,China
[6]Present Address: Risø National Laboratory, Denmark
[7]Present Address: Physics Institute, University of Heidelberg, Heidelberg, Germany
[8]Spokesperson *e-mail: videbaek@bnl.gov*

around $\sqrt{s_{NN}}$ = 7.6 GeV [13] and then decrease slightly with increasing energy. The energy dependence of other observables, like the onset of a plateau for the inverse slope parameter of kaon spectra and a kink in the 4π pion yields normalized to the number of participant nucleons N_{π}/N_{part}, is also used to support the transition to a deconfined phase at $\sqrt{s_{NN}}$ = 7.6 GeV [13]. The gross features of the K/π excitation function can be described in theoretical models, but additional features are needed to describe the data quantitatively. Phenomenologically motivated thermal models can explain the observed behavior with the assumption of a QGP formed in the early stages of the collision [12]. However, more recent thermal models are able to reproduce the 'horn' structure of the excitation function by including higher hadronic resonant states without the assumption of a phase transition [14]. The K^-/π^- ratio has a monotonically increasing energy dependence and is always lower than the K^+/π^+ ratio because of the larger share of strange quarks, which form baryons (mainly Λ's) [13]. From the top SPS energy to the top RHIC energy the K^+/π^+ ratio at mid-rapidity is fairly constant, suggesting that the nuclear medium reaches chemical equilibrium with respect to the production of strange quarks [4].

We present invariant p_T spectra of pions and kaons in central $(0-10\%)$ Au+Au collisions at $\sqrt{s_{NN}}$ = 62.4 GeV measured by the BRAHMS spectrometers[15]. At this energy it is possible by varying the spectrometer angles to achieve an overlap in terms of the baryo-chemical potential (as reflected in the $\bar{p}/p$ ratio) of the RHIC and lower energy SPS results. The data cover the rapidity interval $-0.1 < y < 3.5$, which comes close to the beam rapidity (y_{beam} = 4.2). Total yields deduced from the spectra are used to calculate particle ratios that can be compared to the lower energy SPS results and to theoretical models. The large rapidity coverage allows very different nuclear media to be probed: at mid-rapidity the fireball is dense and the yields of produced anti-hadrons and hadrons are similar ($\pi^-/\pi^+ \sim 1$, $K^-/K^+ \sim 0.85$, $\bar{p}/p \sim 0.45$), while at forward rapidity, in the fragmentation region, we observe a net-baryon rich medium with 4 times smaller meson densities and a 20 times smaller $\bar{p}/p$ ratio. By covering a large interval for important physical parameters (*e.g.* rapidity, particle density, net-baryon density, baryo-chemical potential), these measurements will provide additional constraints to those models that support the conjecture of a phase transition to quark-gluon plasma.

Experimental Setup and Data Analysis

The BRAHMS experiment consists of global event characterization detectors and two spectrometer arms. Collision centrality is determined using a hybrid array of Si strip detectors and plastic scintillator tiles located at the nominal interaction point. The Mid-Rapidity Spectrometer (MRS) and the Forward Spectrometer (FS) are small solid angle spectrometers that can be rotated in the horizontal plane so as together be able to achieve polar angular coverage from 90° to 2.3°. For the present studies, the MRS spectrometer was positioned at 90°, 45° and 40° and the FS at 6°, 4° and 3° at a few magnetic field settings, due to the limited running time.

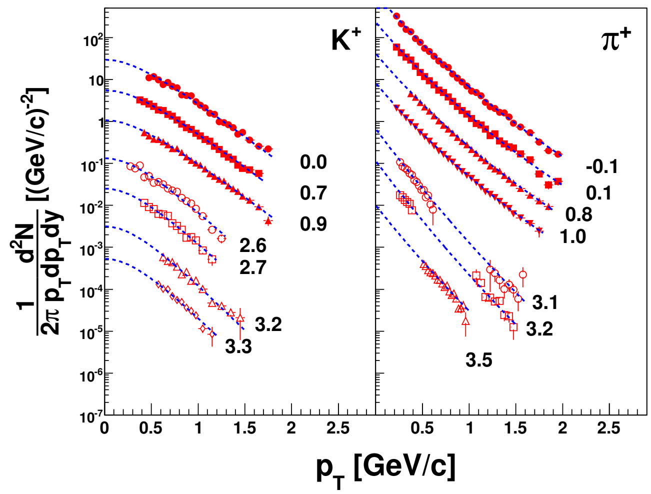

Figure 1: (Color online) Spectra for K^+ (left) and π^+ (right) from 0-10% central Au+Au collisions at $\sqrt{s_{NN}}$ = 62.4 GeV in selected rapidity slices. Each spectrum is multiplied with a factor of 0.2^n for better visibility. For the kaon spectra, the values of n are 0,1,2,3,4,5,6 for the rapidities y = 0.0,0.7,0.9,2.6,2.7,3.2 and 3.3, respectively. For the pion spectra, the values of n are 0,1,2,3,4,5,6 for the rapidities y = -0.1,0.1,0.8,1.0,3.1,3.2 and 3.5, respectively. The fits are m_T exponentials for kaons and p_T power laws for pions. The numbers on the plot indicate the rapidity corresponding to each spectrum. The error bars represent statistical errors.

Particle identification (PID) is achieved in both spectrometers using time-of-flight walls (TOFW in MRS and H2 in FS). In the FS a ring imaging Cherenkov detector (RICH) is used in addition. A detailed description of the technical capabilities of the experimental setup can be found in references [16] and [17]. The identification of charged pions and kaons with the time-of-flight detectors was done by using cuts in (m^2, p) space, where $m^2 = p^2(t_{TOF}^2/L^2 - 1/c^2)$ is determined for a given momentum p by using the time of flight (t_{TOF}) and the track path length(L). Momentum dependent three-σ cuts about the mean m^2 of a given species were applied with the additional condition that the level of contamination from other species at a given m^2 and p is limited to 5% inside the cut. Clean $\pi - K$ separation is achieved up to momenta of 1.5 GeV/c in the MRS and 3 GeV/c in the FS. For higher momenta the 3σ curves overlap and the contamination condition gives asymmetrical cuts in the (m^2, p) space, necessitating the use of momentum dependent cuts and corrections. For the TOFW, the momentum dependent PID corrections ranges from 0 at 1.5 GeV/c up to 20% for pions and 50% for kaons at 2.2 GeV/c. In H2, the same correction ranges from 0 at 3 GeV/c to 10% and 80% at 4.5 GeV/c for pions and kaons, respectively. In the FS, the RICH was used to identify pions and kaons at higher momenta. The pions are separated from kaons by comparing the reconstructed Cherenkov ring radii for momenta with the calculated value for pions in the momentum range of 2.5 to 20 GeV/c. Kaons are identified by the RICH above 10 GeV/c where the RICH efficiency saturates at a value of 97% [17]. Between 4.5 GeV/c and 9 GeV/c an indirect method labels as kaon particles those that give no signal in the RICH but are also not identified as protons in H2. The contamination of kaons with pions unresolved in RICH and

Table 1: dN/dy values for charged pions as a function of rapidity. The given errors are statistical only. The p_T range specified represents the fit range. Fiducial yield is the integrated yield covered by the data.

y	dN/dy power law			dN/dy m_T expo			fiducial yields	
	π^+	π^-	p_T [GeV/c]	π^+	π^-	p_T [GeV/c]	π^+	π^-
-0.20≤y≤0.00	224.0±2.7	232.4±2.9	0.20 - 2.00	195.8±2.2	202.1±2.4	0.20 - 1.00	167.9±2.1	170.4±2.3
0.00≤y≤0.20	231.9±3.2	233.7±2.9	0.20 - 2.00	202.7±2.7	203.6±2.3	0.20 - 1.00	171.7±2.5	171.7±2.1
0.70≤y≤0.90	209.7±2.1	213.1±2.2	0.35 - 1.90	180.7±1.3	182.4±1.4	0.35 - 1.00	99.7±0.6	100.3±0.6
0.90≤y≤1.10	205.5±1.9	214.3±1.9	0.20 - 1.80	178.6±1.2	185.4±1.1	0.20 - 1.00	151.1±1.7	135.9±0.9
3.05≤y≤3.15	57.1±1.9	68.6±3.2	0.25 - 1.60	49.9±0.9	52.2±0.8	0.25 - 1.60	22.4±0.5	24.8±0.5
3.15≤y≤3.25	49.2±1.4	60.5±2.0	0.25 - 1.50	45.8±1.1	53.1±1.2	0.25 - 1.50	11.0±0.4	8.3±0.2
3.40≤y≤3.60	24.8±2.0	24.3±3.7	0.50 - 1.00	20.3±1.2	19.9±1.0	0.50 - 1.00	4.8±0.1	4.9±0.1

Table 2: dN/dy values for charged kaons as a function of rapidity. The errors are statistical only. The p_T range specified represents the fit range. Fiducial yield is the integrated yield covered by the data.

y	dN/dy m_T expo			dN/dy Boltzmann			fiducial yields	
	K^+	K^-	p_T [GeV/c]	K^+	K^-	p_T [GeV/c]	K^+	K^-
-0.15≤y≤0.15	35.6±0.9	30.4±0.8	0.45 - 1.90	33.6±0.8	28.6±0.8	0.45 - 1.90	19.5±0.5	16.6±0.5
0.60≤y≤0.80	33.4±0.4	27.5±0.4	0.35 - 1.80	31.6±0.4	26.0±0.4	0.35 - 1.90	23.9±0.3	15.0±0.2
0.80≤y≤1.00	32.2±0.6	26.7±0.5	0.40 - 1.80	30.1±0.5	26.7±0.5	0.40 - 1.80	19.1±0.4	11.7±0.2
2.55≤y≤2.65	15.2±0.4	8.8±0.3	0.25 - 1.30	14.8±0.4	8.6±0.3	0.25 - 1.30	11.5±0.4	6.6±0.2
2.65≤y≤2.75	14.0±0.4	8.2±0.3	0.35 - 1.20	13.5±0.4	7.9±0.2	0.35 - 1.20	6.6±0.2	4.7±0.14
3.15≤y≤3.25	8.1±0.6	2.9±0.3	0.60 - 1.50	7.5±0.5	2.7±0.3	0.60 - 1.50	2.44±0.12	0.84±0.06
3.25≤y≤3.35	6.8±0.3	2.34±0.14	0.50 - 1.20	6.3±0.3	2.20±0.14	0.50 - 1.20	1.83±0.07	0.75±0.04

protons unresolved in H2 depends on momentum and on relative particle abundances. For K^- the contaminant contribution is estimated to be almost constant at 20% whereas for K^+ it varies from 14% to 40%.

Invariant differential yields, $\frac{1}{2\pi}\frac{d^2N}{p_T dp_T dy}$, were constructed for each spectrometer setting and were corrected for geometrical acceptance, tracking and PID efficiency, contamination, in-flight weak decays and multiple scattering effects by using a Monte Carlo calculation simulating the geometry and tracking of the BRAHMS detector system. The feed-down correction for charged pions originating from the weak decays of K^0_S and Λ was applied as described in reference [4] and amounts to 5% of the measured yield in MRS settings and 7% in FS settings. The feed-down correction was applied directly to the p_T integrated rapidity densities. By merging all of the spectrometer magnet settings, invariant p_T spectra were extracted in several rapidity intervals and fitted with different functions in order to extract the integrated yields (see Fig. 1). We estimate the point-to-point systematic errors to be ≤5% and the systematic errors from normalization, tracking efficiencies and other corrections to be ~8%. The spectrometer acceptances allow measurements down to $p_T = 0.2$ GeV/c for pions and $p_T = 0.25$ GeV/c for kaons, with the absence of lower momentum data contributing to the systematic errors for the integral yield. This uncertainty is largest for pions because of their lowest average p_T. In order to estimate the extrapolation uncertainty, we used both a power law distribution of the form $A(1+p_T/p_0)^{-B}$ and an m_T exponential function to fit the pion spectra. Of these two, the power law distribution gives the best fit to the experimental results over the observed momentum range, and for very low $p_T < 0.1$ GeV/c agrees with the measurements made by the PHOBOS collaboration at $y = 0.8$ [18]. For the m_T exponential function the fit range is limited to $p_T < 1$ GeV/c. The kaon spectra are equally well described by an m_T exponential function, $Ae^{(-m_T/T)}$, and by a Boltzmann distribution. All the presented data are tabulated and available on the BRAHMS website [19].

Results and Discussion

The resulting p_T integrated yields, dN/dy, for pion and kaons are shown in Tables 1 and 2. The dN/dy distributions, taking the statistically weighted average of the two functional forms used in fitting each species, are shown in the upper panel of Fig. 2. The horizontal error bars indicate the width of the rapidity slices and the vertical error bars, smaller than the marker size, are statistical errors. The square brackets below and above each data point indicate the dN/dy values extracted with the employed functionals (see Tables 1 and 2) and serve as an estimate for the systematic errors due to extrapolation to low transverse momentum.

The bottom panel of Fig. 2 shows the rapidity dependence of the average transverse momentum $\langle p_T\rangle$ for pions and kaons. For pions, $\langle p_T\rangle \sim 0.41$ GeV/c at $y = 0$ and decreases to ~ 0.32 GeV/c at $y > 3.0$ while for kaons, $\langle p_T\rangle$ drops from ~ 0.65 GeV/c at $y = 0$ to ~ 0.5 GeV/c at $y = 3.2$. The drop of the averaged transverse momentum at forward rapidity is accompanied by a relatively large decrease in particle densities and in collective models can be explained by the decrease of the collective radial flow velocity.

Figure 3 shows the rapidity-dependent anti-hadron to hadron integrated yield ratios for pions, kaons and protons. The $\bar{p}/p$ ratios are obtained by using the yields presented in reference

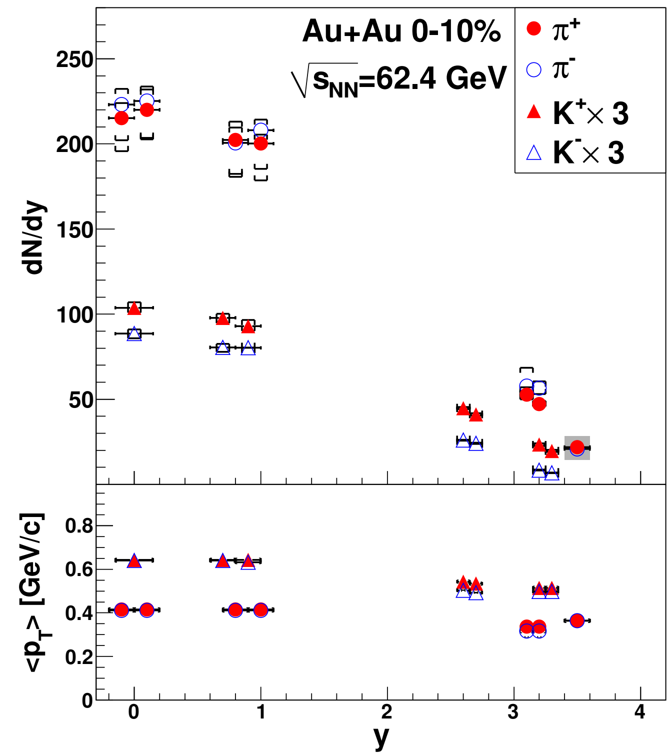

Figure 2: (Color online) Upper panel: dN/dy as a function of rapidity for $\pi^{\pm}$ and $K^{\pm}$ from 0-10% central Au+Au collisions at $\sqrt{s_{NN}}$ = 62.4 GeV. The error bars are statistical. The square brackets below and above each data point indicate the dN/dy values extracted with the selected functionals (see Tables 1 and 2 and text). The experimental uncertainties on the extrapolated yields are below 5% and not shown in the figure, except for the pion yields at y = 3.5 where these amount to ~ 30% and are indicated by the gray box. Bottom panel: $\langle p_T \rangle$ dependence on y. The statistical error bars are covered by the symbols.

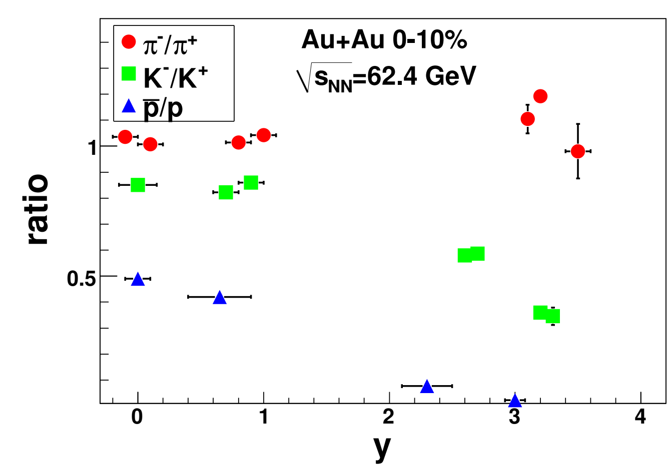

Figure 3: (Color online) Anti-particle to particle ratios as a function of rapidity in 0-10% central Au+Au collisions at $\sqrt{s_{NN}}$ = 62.4 GeV. The error bars are statistical only.

[25]. The baryon yields are not corrected for feed-down from hyperons (see [25]). The π^-/π^+ ratio is approximately equal to unity over the entire rapidity range. The kaon and proton ratios at mid-rapidity ($K^-/K^+ \sim 0.85$, $\bar{p}/p \sim 0.49$) are lower than the corresponding ones measured at the top RHIC energy [24], but they are still characteristic of a high degree of anti-matter to matter equilibration. At forward rapidity we observe a decrease of the kaon ratio to a value of ~ 0.35 at y = 3.3. Possible explanations include the competition between Λ baryons and K^- mesons for the available strange quarks and associated production (e.g., $p + p \rightarrow p + \Lambda + K^+$) which increases the number of positive kaons. Both of these mechanisms depend on the net-baryon content and, consequently, lead to a decrease of the K^-/K^+ ratio at forward rapidity. The $\bar{p}/p$ ratio decreases significantly with rapidity, reaching $\bar{p}/p = 0.077 \pm 0.004(stat.)$ at y=2.3 and $\bar{p}/p = 0.022 \pm 0.001(stat.)$ at $y = 3$.

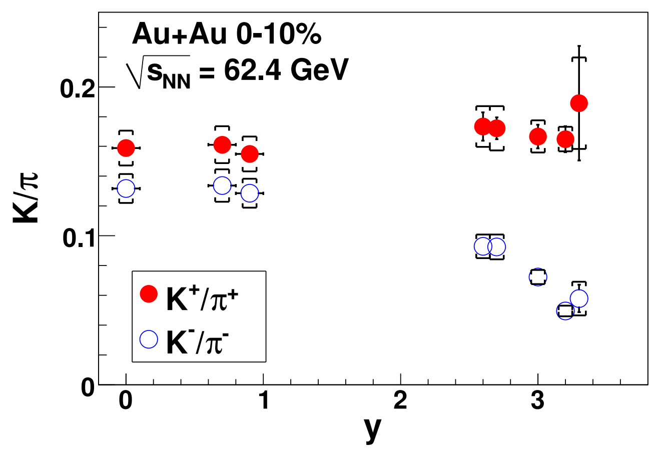

Figure 4: (Color online) Rapidity dependence of the K/π ratios in 0-10% central Au+Au collisions at $\sqrt{s_{NN}}$ = 62.4 GeV. The error bars are statistical errors and the square brackets show the systematic uncertainties due to the yield extrapolation at low p_T.

In Fig. 4 we show the rapidity dependence of the K/π ratio. Because the rapidity intervals where the yields of the two species were extracted are not the same at forward rapidity, we used a linear interpolation procedure between the closest covered points to obtain the meson yields for additional points in rapidity. We checked this procedure by assuming Gaussian rapidity distributions and found very similar results. The K^+/π^+ ratio was found to be 0.159 ± 0.011 at mid-rapidity and is almost constant as a function of rapidity. The K^-/π^- ratio has a value of 0.13 ± 0.01 at mid-rapidity and shows a steep decrease for $y > 2.5$ with a value of ~ 0.05 at $y = 3.2$. The different rapidity dependence of the positive and negative charge K/π ratios is similar to that found in central Au+Au collisions at $\sqrt{s_{NN}}$ = 200 GeV [4] but the difference between the two ratios is three times larger at y=3.

In the following we use calculations with two microscopic transport models for comparison with our data. Ultra-Relativistic Quantum Molecular Dynamics (UrQMD) [20, 21] is the extension of RQMD [10, 11] which was developed to describe physics at AGS and SPS energies. At low energies,

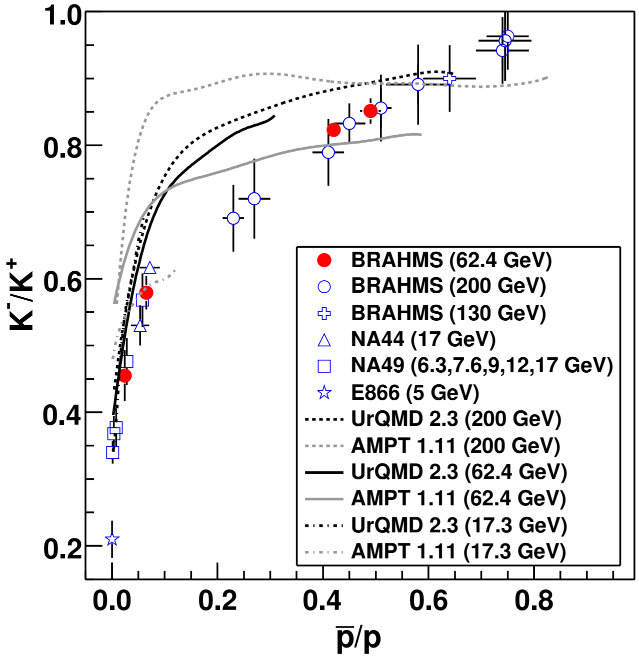

Figure 5: (Color online) K^-/K^+ ratio dependence on the $\bar{p}/p$ ratio. The solid circles are from 0-10% central Au+Au collisions at $\sqrt{s_{NN}}$ = 62.4 GeV obtained in the present work. The open symbols are BRAHMS data from ref. [24] and lower energy data from [3, 29, 30, 31, 32, 33]. The error bars represent statistical and systematic errors. The curves are calculations with UrQMD (black lines) and AMPT (gray lines) for central Au+Au collisions at $\sqrt{s_{NN}}$=200 GeV (dashed lines) and 62.4 GeV (solid lines) and for central Pb+Pb collisions at $\sqrt{s_{NN}}$=17.3 GeV (dot-dashed lines). The curve for the UrQMD calculation at 17.3 GeV is very close to that at 62.4 GeV making it less visible.

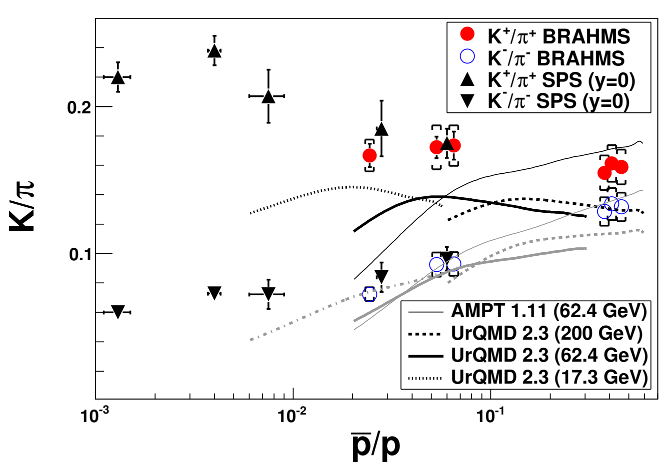

Figure 6: (Color online) K/π ratios as functions of the $\bar{p}/p$ ratio. The circles are data from 0-10% central Au+Au collisions at $\sqrt{s_{NN}}$ = 62.4 GeV and the triangles are results obtained at mid-rapidity in the SPS experiments at different energies [13]. The curves are UrQMD (thick lines) and AMPT (thin lines) calculations for central Au+Au collisions at $\sqrt{s_{NN}}$ = 17.3, 62.4 and 200 GeV. The black curves are for the K^+/π^+ ratio and gray curves are for the K^-/π^- ratio.

$\sqrt{s_{NN}}$ < 5 GeV, it describes the nuclear collisions in terms of interactions between known hadrons and their resonances while at higher energies the dominant mechanism is through the color string excitation. AMPT (A Multiphase Transport Model) [22, 23] is a microscopic model developed for nucleus-nucleus collisions at RHIC and LHC energies. AMPT uses the HIJING model for the initial space-time configuration of the partons and strings. Both UrQMD and AMPT include a Lund-type string fragmentation procedure followed by hadronic rescatterings. The models were run in minimum bias mode with a 0-10% centrality cut placed on the distribution of particles falling in the acceptance of our multiplicity detector ($|\eta| < 2.2$), closely mimicking the experimental conditions.

Figure 5 shows the dependence of the K^-/K^+ ratio on the $\bar{p}/p$ ratio in central nucleus-nucleus collisions at energies ranging from $\sqrt{s_{NN}}$ = 5 to 200 GeV. The data points obtained in this work and from the other RHIC energies are obtained in different rapidity slices, while the SPS and AGS points are obtained at mid-rapidity. Comparing the low and high energy results, we observe a systematic dependence of the K^-/K^+ ratio on the $\bar{p}/p$ ratio. The calculations made with UrQMD(thick lines) and AMPT(thin lines) for central nucleus-nucleus collisions at $\sqrt{s_{NN}}$ = 200, 62.4 and 17.3 GeV do not reproduce quantitatively the dependence of the K^-/K^+ ratio on the $\bar{p}/p$ ratio which seems to be universal over a large energy range. However, UrQMD calculations at the three energies give similar K^-/K^+ ratios for a given $\bar{p}/p$ value. This is most likely due to the thermalization of the system reached via secondary rescatterings, which includes formation, decay and regeneration of many resonances [34].

Figure 6 shows the dependence of the K/π ratios on the $\bar{p}/p$ ratio. Our data points are obtained in different rapidity slices at the same energy, $\sqrt{s_{NN}}$ = 62.4 GeV, while the SPS points are obtained at mid-rapidity in central Pb+Pb collisions at $\sqrt{s_{NN}}$ = 6.3, 7.6, 8.8, 12.3 and 17.3 GeV. In Au+Au collisions at 62.4 GeV, the fragmentation peak is estimated to be in the interval $2.5 < y < 3.3$ [25] with a net-proton density of $\sim$ 30 and $\bar{p}/p$ ratio values at forward rapidity, which are in the same range as those measured at mid-rapidity at $\sqrt{s_{NN}}$ = 12.3 and 17.3 GeV [6]. As in the case of K^-/K^+ ratio, we observe a smooth dependence of the K/π ratios on the $\bar{p}/p$ ratio. The curves show calculations for central Au+Au collisions from UrQMD (thick lines) at $\sqrt{s_{NN}}$ = 17.3, 62.4 and 200 GeV and AMPT (thin lines) at $\sqrt{s_{NN}}$ = 62.4 GeV. None of the models reproduce quantitatively the dependence of the K/π ratios on the $\bar{p}/p$ ratio but qualitatively we observe that UrQMD reproduces the trend of the data.

Figure 7 displays the inverse slope parameters for kaons as a function of the $\bar{p}/p$ ratio. The inverse slope for the highest ratio (0.45) represents the result from a simultaneous fit to the spectra in $0 < y < 1$. Also shown are the mid-rapidity results from SPS. The inverse slopes of the spectra for positive and negative kaons measured at forward rapidity in our dataset are $\sim$ 20 MeV smaller than the ones measured at mid-rapidity in SPS experiments at the same $\bar{p}/p$ ratio. Even though the values are consistent within error bars, the difference suggests that the transverse momenta are not governed by the baryo-chemical

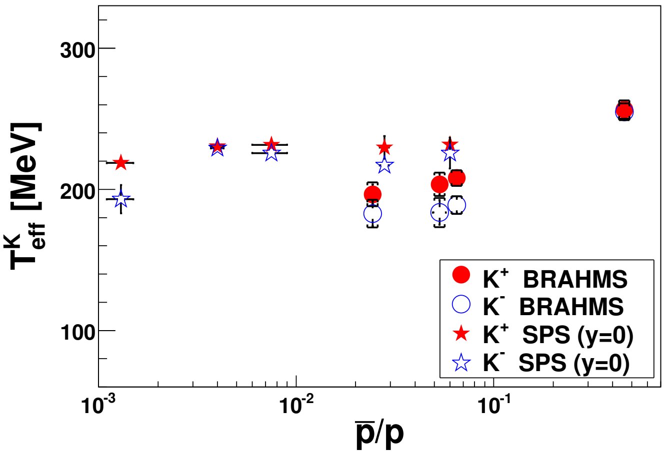

Figure 7: (Color online) Inverse slopes (T_{eff}) for kaons as a function of the $\bar{p}/p$ ratio. The BRAHMS points are from 0-10% central Au+Au collisions at $\sqrt{s_{NN}}$ = 62.4 GeV (this analysis) at different rapidities while the SPS points are from mid-rapidity at different energies [3, 31]. The error bars represent statistical errors, while the square brackets show systematic errors.

potential. The mid-rapidity particle densities for negative pions at SPS at $\sqrt{s_{NN}}$ = 17.3 and 12.3 GeV are approximately two times larger [3] than the negative pion densities at the forward rapidities at $\sqrt{s_{NN}}$ =62.4 GeV. Smaller radial flow from the less dense local system at 62.4 GeV could be the cause of the small difference between inverse slopes. The inverse slopes obtained at forward rapidity are higher for positive kaons than for the negative kaons. This is also observed at mid-rapidity at SPS energies.

In a chemical analysis, the $\bar{p}/p$ ratio has an approximate correspondence with the baryo-chemical potential through the formula $\bar{p}/p = \exp(-2\mu_B/T)$ for a given freeze-out temperature T. Hence if T is the same in the two cases, this would imply that the local system formed at high rapidity at RHIC (62.4 GeV) is chemically equivalent with the system formed at the two highest SPS energies at mid-rapidity, both being controlled by the baryo-chemical potential. The strangeness chemical potential is fixed by the baryo-chemical potential and chemical freeze-out temperature provided that the local net strangeness vanishes. A rapidity dependent baryo-chemical potential μ_B has been suggested in thermal models [26, 27, 28]. The observed dependence of the chemical freeze-out composition in different colliding systems and different rapidities only on the baryo-chemical potential and temperature supports the idea of local chemical equilibration and the existence of a universal $(T-\mu_B)$ freeze-out line.

Summary

In summary, we have measured the transverse momentum spectra and inclusive invariant yields of charged pions and kaons in central Au+Au reactions at 62.4 GeV. The anti-particle/particle ratios for kaons and protons show a steep decrease at forward rapidity. The charge dependence of the K/π ratio at forward rapidities is understood in the framework of microscopic models (*i.e.* UrQMD) as resulting from the associated production in a baryon rich medium. The production mechanisms enhance the fraction of s quarks ending up in hyperons, thus depleting the K^- yield. We observe in central nucleus-nucleus collisions a common dependence of the particle ratios (K/π, K^-/K^+) and kaon spectra inverse slopes on $\bar{p}/p$, which reflects the baryo-chemical potential, whether measured for different energies at mid-rapidity at SPS, or at different rapidities at $\sqrt{s_{NN}}$ = 62.4 GeV. This is consistent with a picture where in nucleus-nucleus collisions, at a given energy, the local fireballs formed at different rapidities freeze out on a $T-\mu_B$ line which coincides with the $T-\mu_B$ freeze-out line previously observed in a wide energy range but only at mid-rapidity. The baryo-chemical potential interval covered at forward rapidity extends to high values and is equivalent to the two highest SPS energies, but not quite high enough to probe the horn structure in the K^+/π^+ ratio excitation function. In the calculations made with UrQMD and AMPT models, K/π ratios are not well reproduced for large baryo-chemical potential found either at high rapidity or mid-rapidity at lower energies although UrQMD seems to reproduce qualitatively the trend of the data. Also, the universal dependence of the K^-/K^+ on the $\bar{p}/p$ ratio is not well explained quantitatively by these microscopic transport models. However the UrQMD model seems to reproduce qualitatively very well this dependence.

Acknowledgements

This work was supported by the Division of Nuclear Physics of the Office of Science of the U.S. Department of Energy under contracts DE-AC02-98-CH10886, DE-FG03-93-ER40773, DE-FG03-96-ER40981, and DE-FG02-99-ER41121, the Danish Natural Science Research Council, the Research Council of Norway, the Polish Ministry of Science and Higher Education (Contract no 1248/B/H03/2009/36), and the Romanian Ministry of Education and Research (5003/1999, 6077/2000). We thank the staff of the Collider-Accelerator Division at BNL and the RHIC Computing Facility for their support to the experiment.

References

[1] L. Ahle *et al.*, E802 Coll., *Phys.Rev.* **C57** (1998) 466
[2] L. Ahle *et al.*, E802 Coll., *Phys.Rev.* **C58** (1998) 3523
[3] S.V. Afanasiev *et al.*, NA49 Coll., *Phys.Rev.* **C66** (2002) 054902
[4] I.G. Bearden *et al.*, BRAHMS Coll., *Phys.Rev.Lett.* **94** (2005) 162301
[5] L. Ahle *et al.*, E802 Coll., *Phys.Rev.* **C59** (1999) 2173
[6] C. Alt *et al.*, NA49 Coll., *Phys.Rev.* **C73** (2006) 044910
[7] I.G. Bearden *et al.*, BRAHMS Coll., *Phys.Rev.Lett.* **93** (2004) 102301
[8] L. Ahle *et al.*, E866 and E917 Coll., *Nucl.Phys.* **A638** (1998) 57C
[9] S. Ahmad *et al.*, E891 Coll., *Phys.Lett.* **B382** (1996) 35
[10] H. Sorge, H. Stöcker and W. Greiner, *Ann.Phys. (NY)* **192** (1989) 266
[11] H. Sorge, H. Stöcker and W. Greiner, *Nucl.Phys.* **A498** (1989) 567
[12] M. Gazdzicki and M. Gorenstein, *Acta Phys.Polon.* **B30** (1999) 2705
[13] M. Mitrovski *et al.*, NA49 Coll., *J.Phys.* **G32** (2006) S43
[14] A. Andronic, P. Braun-Munzinger, J. Stachel, *Phys.Lett.* **B678** (2009) 516
[15] I. Arsene *et al.*, BRAHMS Coll., *Nucl.Phys.* **A757** (2005) 1
[16] M. Adamczyk *et al.*, BRAHMS Coll., *Nucl.Instr.Meth.* **A499** (2003) 437
[17] R. Debbe *et al.*, *Nucl.Instr.Meth.* **A570** (2007) 216
[18] B.B. Back *et al.*, PHOBOS Coll., *Phys.Rev.* **C77** (2007) 024910

[19] http://www.rhic.bnl.gov/brahms/WWW/publications.html
[20] S.A. Bass *et al.*, *Prog.Part.Nucl.Phys.* **41** (1998) 225
[21] M. Bleicher *et al.*, *J.Phys.* **G25** (1999) 1859
[22] B. Zhang *et al.*, *Phys.Rev.* **C61** (2000) 067901
[23] Z.-w. Lin *et al.*, *Nucl.Phys.* **A698** (2002) 375
[24] I.G. Bearden *et al.*, BRAHMS Coll., *Phys.Rev.Lett.* **90** (2003) 10
[25] I.C. Arsene *et al.*, BRAHMS Coll., *Phys.Lett.* **B677** (2009) 267
[26] F. Becattini, J.Cleymans, *J.Phys.* **G34** (2007) S959
[27] B. Biedron, W. Broniowski, *J.Phys.* **G35** (2008) 044011; *Phys.Rev.* **C76** (2007) 054905
[28] L. A. Stiles, M. Murray, *arXiv:*nucl-ex/0601039v1
[29] L. Ahle *et al.*, E866 Coll., *Phys.Rev.Lett.* **81** (1998) 2650
[30] M.van Leeuwen *et al.*, NA49 Coll., *Nucl.Phys.* **A715** (2003) 161
[31] C. Alt *et al.*, NA49 Coll., *Phys.Rev.* **C77** (2008) 024903
[32] C. Alt *et al.*, NA49 Coll., *Phys.Rev.* **C73** (2006) 044910
[33] I.G. Bearden *et al.*, NA44 Coll., *Phys.Rev.* **C66** (2002) 044907
[34] L. V. Bravina *et al.*, *Phys.Rev.* **C78** (2008) 014907